

Iowa State University

From the Selected Works of Valery I. Levitas

2002

Three-dimensional Landau theory for
multivariant stress-induced martensitic phase
transformations. I. Austenite \leftrightarrow martensite

Valery I. Levitas, *Texas Tech University*

Dean L. Preston, *Los Alamos National Laboratory*



Available at: https://works.bepress.com/valery_levitas/44/

Three-dimensional Landau theory for multivariant stress-induced martensitic phase transformations. I. Austenite \leftrightarrow martensite

Valery I. Levitas^{1,*} and Dean L. Preston²¹*Texas Tech University, Department of Mechanical Engineering, Lubbock, Texas 79409-1021*²*Applied Physics Division, Los Alamos National Laboratory, Los Alamos, New Mexico 87545*

(Received 13 February 2002; published 23 October 2002)

A three-dimensional Landau theory of stress-induced martensitic phase transformations is presented. It describes transformations between austenite and martensitic variants and transformations between martensitic variants. The Landau free energy incorporates all temperature-dependent thermomechanical properties of both phases. The theory accounts for the principal features of martensitic transformations in shape memory alloys and steels, namely, stress-strain curves with constant transformation strain and constant, or weakly temperature dependent, stress hysteresis, as well as nonzero tangent elastic moduli at the phase transformation point. In part I, the austenite \leftrightarrow martensite phase transformation is treated, while transformations between martensitic variants are considered in part II.

DOI: 10.1103/PhysRevB.66.134206

PACS number(s): 64.60.-i

I. INTRODUCTION

Landau theory¹ is a phenomenological framework that originated as a description of second-order (continuous) phase transformations. Although the conventional Landau approach is strictly valid only for continuous phase transformations, Landau theory has been generalized to encompass first-order phase transformations, in particular displacive reconstructive transitions, which include martensitic phase transformations.

The basic ingredients of a Landau model are an order parameter η , which encodes the atomic configurations through the transformation, and the thermodynamic potential G , which is a function of the order parameter. See Ref. 2 for an excellent overview of modern Landau theory.

In Ginzburg-Landau theory, a gradient term is included in the total energy to account for interface surface energy

$$G_{\text{GL}} = G + 0.5 \sum_{k=1}^n \nabla \eta_k \cdot \boldsymbol{\beta}_k \cdot \nabla \eta_k. \quad (1)$$

The $\boldsymbol{\beta}_k$ are positive definite second-rank tensors. Since the driving force to change η_k equals $-\delta G_{\text{GL}}/\delta \eta_k$, the kinetic equations for η_k are given by³⁻⁶

$$\begin{aligned} \frac{\partial \eta_k}{\partial t} &= - \sum_{p=1}^n L_{kp} \frac{\delta G_{\text{GL}}}{\delta \eta_p} + \xi_k \\ &= - \sum_{p=1}^n L_{kp} \left(\frac{\partial G}{\partial \eta_p} - \boldsymbol{\beta}_p : \nabla \nabla \eta_p \right) + \xi_k. \end{aligned} \quad (2)$$

Here L_{kp} are positive definite kinetic coefficients and ξ_k is the noise due to thermal fluctuations which satisfies the dissipation-fluctuation theorem.

We construct a Landau free energy that describes strong first-order martensitic phase transformations (PT's) in steels and shape memory alloys (SMA's). Hence the transformation strain must be temperature independent, and the stress hysteresis must be constant or only weakly temperature dependent. Further, the tangent elastic moduli at the PT point are

required to be nonzero. Finally, the theory should accommodate all of the thermomechanical properties of both phases. We now discuss these required features of our Landau free energy in some detail.

Deformation of the crystal lattice of the high-temperature phase, the austenite (A), into the low temperature phase, the martensite (M), can be described in the small strain approximation by the transformation strain tensor $\boldsymbol{\epsilon}_t$ (also called Bain strain⁷ or spontaneous strain.^{8,9}) Due to the symmetry of the crystal lattice, there are a finite number n of crystallographically equivalent variants of martensite. All martensitic variants M_i , $i=1,2,\dots,n$, have the same components of the transformation strain tensor in their respective crystallographic bases. A list of transformation strain tensors for transformations between various crystal lattices can be found in Ref. 10. Maximal components of the transformation strain tensor are of order 0.1. In contrast to some ferroelastics,⁹ for which the transformation strain can increase significantly as the temperature is decreased, the transformation strain is constant for SMA and steels. A small deformation of the martensitic crystal lattice under temperature variation can be described by a thermal expansion tensor of M that has the same order of magnitude as for A ($\alpha \sim 10^{-5}$ 1/K).

Phase transformations in some classes of materials [see Ref. 9 for Nb_3Sn , BiVO_4 , LaNbO_4 , $(\text{KBr})_{0.27}(\text{KCN})_{0.73}$, KH_2PO_4 , TbVO_4 , and Ref. 11 for V_3Si , Nb_3Sn , and InTe alloys) occur at vanishing tangent elastic modulus E_t corresponding to the transformation strain. The transformation strains in such materials are usually small, and the PT are close to second order. In contrast, martensitic PT occur at nonzero E_t in both A and M . Examples include Cu-based alloys:¹² Fe-33.7% Ni, Fe-5.9% Ni-4.4% Mn-0.48% C steels, Co - 32.5% Ni and Cu - 14.3% Al-5.8% Ni alloys,¹¹ CuZnAl,¹³ and TiNi alloys.¹⁴ Consequently, the transition mechanism cannot be attributed to phonon instability, and the soft-mode approach¹⁵ cannot be applied.

Stress hysteresis in SMA is typified by a weak dependence on temperature.^{14,16} For example, in Cu-Zn-Al alloys the stress hysteresis is constant for a temperature variation

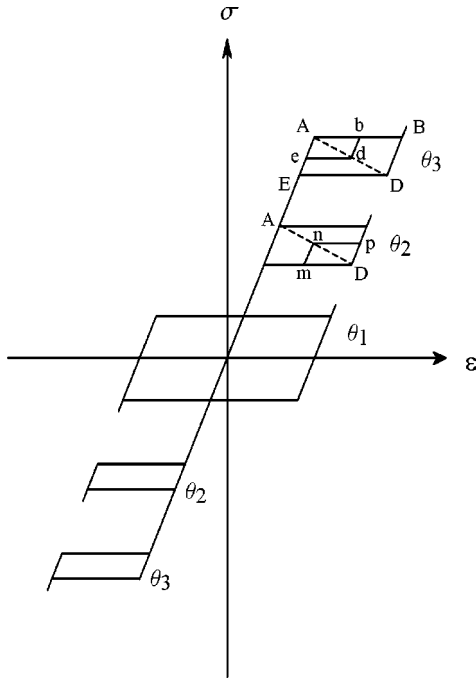


FIG. 1. Schematic stress-strain curves for shape memory alloys at various temperatures $\theta_1 < \theta_2 < \theta_3$. The behavior is pseudoplastic at θ_1 and pseudoelastic at θ_2 and θ_3 . The constant transformation strain and the weak temperature dependence of stress hysteresis for pseudoelastic behavior is typical.

from 12° to 78°C; the corresponding variation in the initiation stress for the $A \rightarrow M$ PT is 10 to 120 MPa (Ref. 17) (see Ref. 13 for similar results). This is again in contrast to some ferroelastics⁹ for which the shape of the hysteresis loop remains invariant, but the transformation strain and the difference between the stresses for direct and reverse PT, i.e., the stress hysteresis, grows significantly with decreasing temperature, starting from zero at the transition temperature.

A generic stress (σ)-strain (ε) curve for monocrystalline SMA under cyclic loading¹³ is shown in Fig. 1. The $A \rightarrow M$ ($M \rightarrow A$) transformation takes place at the higher (lower) stress modulus in each hysteresis loop. The volume fraction of M varies from 0 to 1 along the path from A to B , but decreases from 1 to 0 along the path from D to E . If unloading starts before the direct PT is complete, then on the line bd (point d lies on the diagonal AD) the $A+M$ mixture responds elastically without further phase transformation, and the curve de corresponds to the $M \rightarrow A$ PT. If we interrupt the reverse PT at some point m , then along the line mn the $A+M$ mixture deforms elastically, and along the line np the $A \rightarrow M$ PT occurs. The diagonal AD is the thermodynamically unstable equilibrium stress-strain curve. The high-temperature behavior, characterized by the occurrence of direct and reverse PT at stresses of the same sign and zero residual transformation strain at zero stress, is called pseudoelastic. At low temperatures, where stress reversal is necessary to induce the reverse PT and there is a residual transformation stress at zero strain, the behavior is referred to as pseudoplastic.

One class of Landau theories of martensitic PT is based

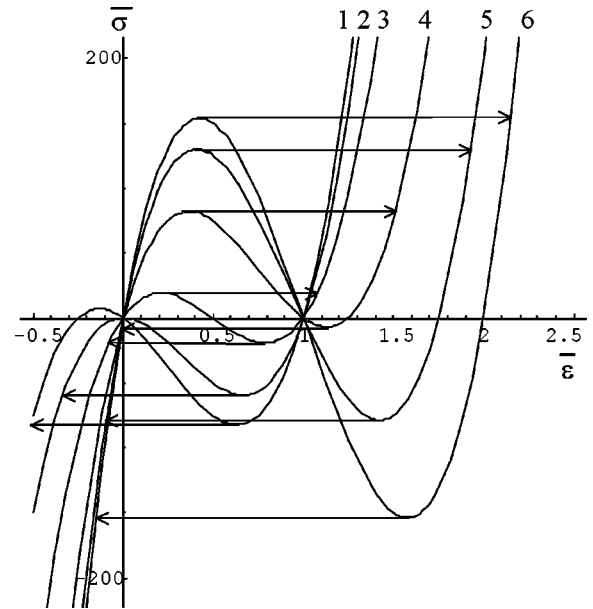


FIG. 2. Stress-strain curves at six temperatures for the 2-3-4 potential proposed in Ref. 21 at $\theta_e = 150$ K and $\theta_c = 50$ K: (1) $\theta = 0$ K; (2) $\theta = 50$ K; (3) $\theta = 150$ K; (4) $\theta = 300$ K; (5) $\theta = 400$ K; (6) $\theta = 500$ K.

on nonconvex Helmholtz free-energy polynomials in the strain ε : $F(\varepsilon) = a\varepsilon^2 + b\varepsilon^4 + c\varepsilon^6$ (Ref. 18) (in Refs. 19, 20 a Gibbs potential $G = F - \sigma\varepsilon$ is used which gives the same results) or $F(\varepsilon) = a\varepsilon^2 + b\varepsilon^3 + c\varepsilon^4$.²¹⁻²⁴ The elastic constants a , b , and c are functions of the temperature θ ; usually $a = a_0(\theta - \theta_c)$, where θ_c is the critical temperature at which the stress-free high-temperature phase loses its thermodynamic stability. Stress-strain curves $\sigma = \partial F / \partial \varepsilon$ at different temperatures for the 2-4-6 potential are analyzed in detail in Ref. 18 with the goal of applying them to SMA. This is the only work we know of where σ - ε curves are studied for a Landau theory. In dimensionless form the stress-strain relation for the 2-4-6 potential is $\bar{\sigma} = 6\bar{\varepsilon}^5 - 4\bar{\varepsilon}^3 + 2(t + \frac{1}{4})\bar{\varepsilon}$, where t is the dimensionless temperature. The transformation strain and stress hysteresis grow monotonically from zero at $t = 1/4$ with decreasing temperature, and both phases lose their stability at zero tangent elastic moduli. Similar behavior is seen in the one-dimensional version of the 2-3-4 potential.^{8,9,23,24} Olson and Cohen²¹ defined coefficients in a 2-3-4 potential so that it has stationary points at $\varepsilon = 0$ and $\varepsilon = g$, where g is a constant. Their stress-strain curves $\bar{\sigma} = 2(\theta - \theta_c)\bar{\eta} - 2(\theta + 2\theta_e - 3\theta_c)\bar{\eta}^2 + 4(\theta_e - \theta_c)\bar{\eta}^3$ (θ_e is the temperature of thermodynamic equilibrium between stress-free A and M , $\bar{\eta} = \varepsilon/g$, and $\bar{\sigma}$ is proportional to the stress) are plotted at six temperatures in Fig. 2. These curves describe qualitatively the pseudoplastic regime, but because the stress is always zero at $\varepsilon = 0$ and $\varepsilon = g$ the pseudoelastic regime, where $M \rightarrow A$ PT occurs at unloading, is not described at all. Both phases lose their stability at zero tangent elastic moduli, and hysteresis and transformation strain are strongly temperature dependent. This behavior is generic for free-energy polynomials in the strain.

An alternative description of first order PT is provided by

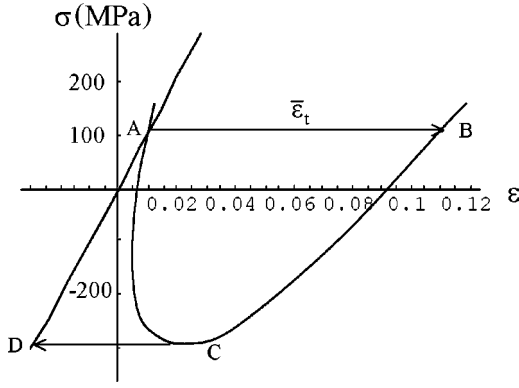


FIG. 3. Equilibrium stress-strain curve described by Eqs. (3)–(5) for $k=2$, $E=10^4$ MPa, $\varepsilon_0=0.005$, $\varepsilon_s=0.01$, $\bar{\varepsilon}_t=0.1$, and arbitrary d .

a Landau polynomial in some order parameter η with linear or quadratic coupling to the strain tensor: $F = a\eta^2 + b\eta^4 + c\eta^6 + E\varepsilon^2/2 - d\eta^k\varepsilon$, where $k=1, 2$ and d is the striction coefficient. The order parameter is usually related to atomic shuffles; deformation of the crystal lattice is considered a secondary order parameter. The thermodynamic equilibrium conditions are

$$\partial F/\partial \eta = 2a\eta + 4b\eta^3 + 6c\eta^5 - kd\eta^{k-1}\varepsilon = 0, \quad (3)$$

$$\sigma = \partial F/\partial \varepsilon = E\varepsilon - d\eta^k = E(\varepsilon - \varepsilon_t), \quad (4)$$

$$\varepsilon_t := d\eta^k/E. \quad (5)$$

Due to coupling with the strain, the order parameter produces spontaneous transformation strain ε_t .^{3,4,8,9,25–27}

A $k=1$ polynomial^{5,9} was employed to model the cubic to tetragonal transformation in FePd alloy,⁶ and a three-dimensional $k=1$ theory was used to model martensitic PT in SMA and steel.⁵ If $\varepsilon > 0$, then the solution $\eta=0$ of the thermodynamic equilibrium condition (3) disappears, i.e., the parent phase at any temperature is unstable at any prescribed strain and the PT starts immediately with straining. The equilibrium η and transformation strain defined by Eqs. (3) and (5) grow monotonically with increasing strain. So a linear coupling of η to the strain tensor ($k=1$) is unsuitable for the description of martensitic PT. The same conclusion is reached if one uses the 2-3-4 polynomial instead of the 2-4-6 potential.⁵

For the more common case $k=2$,^{3,4,25–27} $\eta=0$ (corresponding to A) is always a solution of Eq. (3). Two other solutions appear when $\varepsilon \geq \varepsilon_0 = (a - b^2/3c)/d$. One finds that the stable solution for the transformation strain grows without bound as strain increases. When $\varepsilon \geq \varepsilon_s = a/d$ the solution $\eta=0$ corresponds to a maximum of the free energy, i.e., it is unstable to infinitesimal perturbations. The equilibrium stress-strain curve $\sigma = E(\varepsilon - \varepsilon_t)$ is shown in Fig. 3. Loss of stability of A at $\varepsilon = \varepsilon_s$ (point A) does not occur at zero tangent elastic modulus, and this model describes well the experimental relation between the elastic constant in the direction of the transformation shear and the zone-boundary frequency of the associated phonon branch at the phase equi-

librium temperature for Cu-based alloys.¹² However, the loss of stability of martensite does occur at zero tangent elastic modulus²⁶ (point C), and the forward (AB) and reverse (CD) transformation strains are unequal, which is at variance with observation. After A loses stability, both strain and stress decrease along the unphysical equilibrium stress-strain curve AC. Moreover, the $k=2$ potential cannot describe pseudoelastic behavior, only the pseudoplastic regime can be modeled. Macroscopic stress-strain curves based on this model and calculated in Refs. 3, 4 also exhibit pseudoplastic behavior only.

A notable drawback of the above models is that the elastic constants a , b , and c of A completely determine the elastic properties of M. This is not the case in general. For example, the Young's moduli of A and M are approximately the same for CuZnAl alloys¹³ and differ by a factor of four for TiNi alloys.¹⁴ These models do not have a sufficient number of degrees of freedom to incorporate the thermoelastic properties (elastic moduli of second, third, and higher order, thermal expansion coefficients, and difference in thermal parts of free energy) of both A and M, or the transformation characteristics (transformation strain and stress hysteresis) and their temperature dependences.

There are more general models which account for atomic shuffles and involve more complex couplings with elastic strain.^{25,28–30} Nevertheless, they also cannot account for the material properties of both phases or the transformation characteristics of strongly first-order martensitic PT.

Known three-dimensional multivariant theories^{3,4,19,20,23,24,31} are simple generalizations of the above one-dimensional models and they do not overcome their drawbacks. New problems arise because of the necessity to describe the transformation of one martensitic variant into another. We do not know of any paper where this problem has been studied analytically.

It seems that the theory advocated in Ref. 31 contains enough parameters to encompass the transformation characteristics and the material parameters of both phases. However, in one dimension it reduces to a 2-3-4 polynomial in the strain, so it has all of the shortcomings of this potential. A three-dimensional theory³² that generalizes the 2-4-6 potential¹⁸ discussed above by including additional parameters still suffers from the deficiencies of the 2-4-6 potential. Group representation theory was used in each case^{31,32} to derive quite complex polynomials which may have unphysical minima. The simplest possible polynomial which satisfies all reasonable requirements (see Ref. 33) is preferable.

There has been significant progress in numerical modeling of microstructure formation during martensitic PT based on Landau-Ginzburg theory. A number of two-dimensional^{19,20} and three-dimensional calculations^{3–5,34} have been performed. Despite the drawbacks discussed above, numerical simulations based on existing models predict multivariant microstructures in qualitative agreement with photomicrographs. The salient features of the microstructure are apparently controlled by the elastic-energy-minimization constraint on the self-organization of the martensitic domains; material properties and transformation characteristics presumably affect only the details in the mi-

crostructure. Agreement of the simulations with the data may be attributed in part to the similarities among experimentally observed microstructures (compare Ref. 9 for ferroelastics and Ref. 35 for SMA).

All martensitic PT (even thermally induced) are affected or governed by internal stresses arising from transformation strain and crystal defects (dislocations and point defects). Any Landau potential generates stress-strain relationships, equilibrium diagrams, and transformation diagrams under general three-dimensional loading. However, no known Landau potential is consistent with experimental stress-strain relationships. Generally, the predictions of Landau theory agree only qualitatively with observation. Nevertheless, the Landau potential developed in this two-part paper does describe the typical features of experimental stress-strain curves.

In Sec. II we develop our Landau model of austenite-martensite transformations. The simplest case, namely equal elastic compliances for austenite and martensite, and zero thermal stresses, is considered in Sec. II A. In Sec. II B we present the general case, including higher-order elastic compliances. Our concluding remarks for part I are made in Sec. III. In part II the Landau free energy constructed in part I is extended to incorporate an arbitrary number of martensitic variants, hence it accounts for PT between austenite and martensitic variants and transformations between martensitic variants.

Direct tensor notations are used throughout this paper. Vectors and tensors are denoted in boldface type; $\mathbf{m}\mathbf{n}$ is the dyadic product of vectors \mathbf{m} and \mathbf{n} , $\mathbf{A}\cdot\mathbf{B}=(A_{ij}B_{jk})$ and $\mathbf{A}:\mathbf{B}=A_{ij}B_{ji}$ are the contraction of tensors over one and two indices, $|\mathbf{A}|:=(\mathbf{A}:\mathbf{A})^{1/2}$ is the modulus of tensor \mathbf{A} , and $:=$ means equal by definition. The indices 1 and 2 denote the values in A and M respectively.

II. LANDAU MODEL OF AUSTENITE \leftrightarrow MARTENSITE

We assume that for the three-dimensional case all material properties (elastic moduli tensors of second, third, and higher order, thermal expansion tensors, and thermal parts of the free energy) of both phases, the transformation strain tensor, and all temperature dependences, are known for a given material. Transformation characteristics, such as the critical temperature θ_c for the formation of martensite, the relation between the stress tensor and the temperature at which A and M_i lose their stability, or are in thermodynamic equilibrium, and the potential barriers are also known from experiment or atomistic calculations. Our goal is to find the simplest expression for the Gibbs potential that describes the $A\leftrightarrow M_i$ and $M_i\leftrightarrow M_j$ (part II) PT for any type of symmetry of A and M and includes all of this information.

The following approach is followed in this section. Shuffles are neglected or excluded by minimization of free energy. We decompose the total strain tensor into elastic and transformational parts. The magnitude of the transformation strain tensor is uniquely related to the order parameter η , which varies from 0 in A to 1 in M . We require that the material be either A or M in thermodynamic equilibrium at any temperature and stress tensor. This translates into the

requirement that the Gibbs potential at any temperature and for any stress field has extrema at $\eta=0$ and $\eta=1$. We use a 2-3-4 polynomial for the thermal part of the Gibbs energy (which is usual) and for the transformation strain (which is new) and easily satisfy this requirement. Changes in the second- and higher-order elastic compliance tensors and the thermal strain tensor during the PT are taken into account. Analysis of the model shows that we can include complete material property information and describe all characteristic features of martensitic PT. In part II, this approach will be extended to the general multivariant case.

Our assumed decomposition of the total strain into elastic and transformational parts is valid only for small strains. At finite strain, this additive decomposition breaks down—one has to use multiplicative decomposition of the deformation gradient into elastic and transformational parts and take into account finite rotations.³⁶ Formal problems then arise, similar to those encountered in finite elastoplasticity.³⁷ We will limit ourselves in this paper to the small strain approximation.

A. η -independent elastic compliance and zero thermal strain

The strain tensor $\boldsymbol{\varepsilon}$ is decomposed into elastic $\boldsymbol{\varepsilon}_e$ and transformational $\tilde{\boldsymbol{\varepsilon}}_t(\eta):=\boldsymbol{\varepsilon}_t\varphi(\eta)$ parts

$$\boldsymbol{\varepsilon}=\boldsymbol{\varepsilon}_e+\boldsymbol{\varepsilon}_t\varphi(\eta), \quad (6)$$

where $\boldsymbol{\varepsilon}_t$ is the transformation strain tensor at thermodynamic equilibrium in the martensitic phase ($\boldsymbol{\varepsilon}_t$ is determined by crystallography), η is the order parameter ($0\leq\eta\leq 1$), and φ is a monotone function for which $\varphi(0)=0$ and $\varphi(1)=1$. As η varies from 0 to 1, the transformation strain tensor varies from $\mathbf{0}$ to its final value $\boldsymbol{\varepsilon}_t$. The order parameter η is uniquely related to the magnitude of the transformation strain $|\tilde{\boldsymbol{\varepsilon}}_t|$ normalized by its maximum value $|\boldsymbol{\varepsilon}_t|$.

We assume for simplicity that the thermal strain is zero and that the elastic moduli of the austenite and martensite are equal (these assumptions are relaxed below) and write the specific (per unit volume) Gibbs free energy in the form

$$G=-\boldsymbol{\sigma}:\boldsymbol{\lambda}:\boldsymbol{\sigma}/2-\boldsymbol{\sigma}:\boldsymbol{\varepsilon}_t\varphi(\eta)+f(\theta,\eta), \quad (7)$$

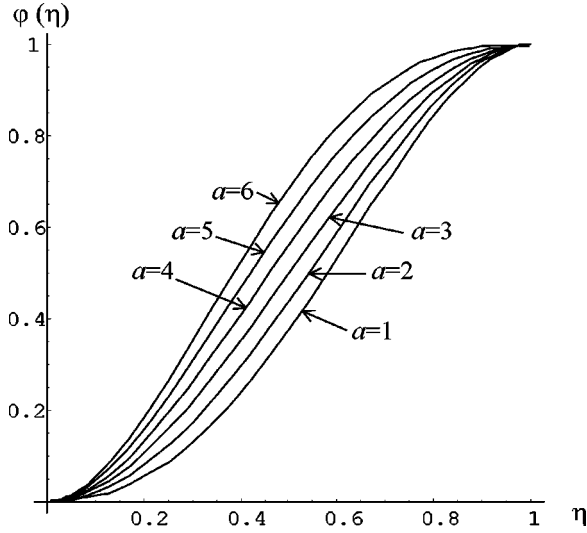
where $\boldsymbol{\sigma}$ is the stress tensor, $\boldsymbol{\lambda}$ is the fourth-rank elastic compliance tensor, θ is the temperature, and f is the thermal or chemical (stress-independent) part of the free energy. Then

$$\boldsymbol{\varepsilon}=-\partial G/\partial\boldsymbol{\sigma}=\boldsymbol{\lambda}:\boldsymbol{\sigma}+\boldsymbol{\varepsilon}_t\varphi(\eta), \quad (8)$$

which is consistent with Eq. (6). Our goal is to find the functions $\varphi(\eta)$ and $f(\theta,\eta)$ satisfying the following three conditions:

$$(1)\varphi(0)=0 \text{ and } \varphi(1)=1; \quad f(\theta,1)-f(\theta,0)=\Delta G^\theta(\theta). \quad (9)$$

The conditions on φ imply $\tilde{\boldsymbol{\varepsilon}}_t(0)=\mathbf{0}$ and $\tilde{\boldsymbol{\varepsilon}}_t(1)=\boldsymbol{\varepsilon}_t$. $\Delta G^\theta(\theta)$ is the difference between the thermal parts of the Gibbs free energies of the martensitic and austenitic phases as determined experimentally. It is clear that $f(\theta,0)$

FIG. 4. The function $\varphi(\eta)$ at various a .

$=G_1^\theta(\theta)$, however for the description of PT without loss of generality we can put $f(\theta, 0) = 0$.

(2) The free energy G has extrema at A and M

$$\frac{\partial G(\boldsymbol{\sigma}, \theta, \hat{\eta})}{\partial \eta} = 0 \Rightarrow \frac{\partial \varphi(\hat{\eta})}{\partial \eta} = \frac{\partial f(\theta, \hat{\eta})}{\partial \eta} = 0, \quad \hat{\eta} = 0, 1. \quad (10)$$

(3) The function $\varphi(\eta)$ is monotone for $0 \leq \eta \leq 1$.

If we choose $\varphi(\eta)$ and $f(\eta)$ to be 2-3-4 polynomials, then conditions (1)–(3) are satisfied by the functions

$$\begin{aligned} \varphi(\eta) &= a\eta^2 + (4-2a)\eta^3 + (a-3)\eta^4, \quad 0 < a < 6, \\ f(\theta, \eta) &= A\eta^2 + (4\Delta G^\theta - 2A)\eta^3 + (A - 3\Delta G^\theta)\eta^4, \end{aligned} \quad (11)$$

where a and A are material parameters. The function $\varphi(\eta)$ has no extremum on the interval $0 \leq \eta \leq 1$ for $0 \leq a \leq 6$; we include the end points $a=0$ and $a=6$ where infinite stress is required to initiate direct and reverse PT [see Eq. (22)]. The function $\varphi(\eta)$ for various a is shown in Fig. 4. By rescaling η and energy, the potential can be put in the form $\tilde{G} = K\tilde{\eta}^2 + \tilde{\eta}^3 + \tilde{\eta}^4$. However, since K depends in a complex way on stresses and ΔG^θ , and our goal is to study the effect of stresses on the PT, we work directly with Eqs. (7) and (11). The difference between the Gibbs potentials of the A and M phases, which is the thermodynamic driving force for the $A \rightarrow M$ PT, is $G(\boldsymbol{\sigma}, \theta, 0) - G(\boldsymbol{\sigma}, \theta, 1) = \boldsymbol{\sigma} \cdot \boldsymbol{\varepsilon}_i - \Delta G^\theta$. The thermodynamic equilibrium condition $\partial G / \partial \eta = 0$ has the three roots

$$\eta_1 = 0; \quad \eta_2 = 1;$$

$$\eta_3 = \frac{1}{2}(A - a\boldsymbol{\sigma} \cdot \boldsymbol{\varepsilon}_i) / [A - 3\Delta G^\theta - (a-3)\boldsymbol{\sigma} \cdot \boldsymbol{\varepsilon}_i]. \quad (12)$$

The first two roots correspond to austenitic and martensitic minima (if these phases are metastable). If the third root is between 0 and 1, it corresponds to the maximum of

$G(\boldsymbol{\sigma}, \theta, \eta)$, which represents the activation barrier for the $A \rightarrow M$ PT. The barrier height is

$$\begin{aligned} &G(\boldsymbol{\sigma}, \theta, \eta_3) - G(\boldsymbol{\sigma}, \theta, 0) \\ &= [A - \boldsymbol{\sigma} \cdot \boldsymbol{\varepsilon}_i a - 4(\Delta G^\theta - \boldsymbol{\sigma} \cdot \boldsymbol{\varepsilon}_i)]\eta_3^3/2. \end{aligned} \quad (13)$$

The activation barrier for $M \rightarrow A$ is $G(\boldsymbol{\sigma}, \theta, \eta_3) - G(\boldsymbol{\sigma}, \theta, \eta_2)$, which can be obtained by adding $G(\boldsymbol{\sigma}, \theta, 0) - G(\boldsymbol{\sigma}, \theta, 1) = \boldsymbol{\sigma} \cdot \boldsymbol{\varepsilon}_i - \Delta G^\theta$ to Eq. (13). The inequalities $\partial^2 G / \partial \eta^2 \leq 0$ at $\eta = 0$ and $\eta = 1$ are conditions for the loss of A and M stability. They are the $A \rightarrow M$ and $M \rightarrow A$ PT criteria [rather than the phase equilibrium condition $G(\boldsymbol{\sigma}, \theta, 0) = G(\boldsymbol{\sigma}, \theta, 1)$]

$$A \rightarrow M: \quad \boldsymbol{\sigma} \cdot \boldsymbol{\varepsilon}_i \geq \frac{A}{a}, \quad M \rightarrow A: \quad \boldsymbol{\sigma} \cdot \boldsymbol{\varepsilon}_i \leq \frac{6\Delta G^\theta - A}{6 - a}. \quad (14)$$

The criteria (14) also follow from the conditions $\eta_3 \leq 0$ and $\eta_3 \geq 1$, in which case η_3 corresponds to a minimum of G and η_1 (or η_2) to a maximum, and the barrier for the PT disappears. For temperature-induced PT ($\boldsymbol{\sigma} = 0$) Eqs. (14) reduce to $A \leq 0$ ($A \rightarrow M$) and $A \leq 6\Delta G^\theta$ ($M \rightarrow A$). If the difference between the specific heats of the phases at zero stress $\Delta \nu$ is independent of temperature, then it is easy to obtain (see, e.g., Refs. 13,36)

$$\begin{aligned} \Delta G^\theta &= z(\theta - \theta_e) - \Delta \nu \theta (\ln \theta / \theta_e - 1) - \Delta \nu \theta_e, \\ z &= -\Delta s_e > 0. \end{aligned} \quad (15)$$

Here θ_e is the equilibrium temperature [$\Delta G^\theta(\theta_e) = 0$] and Δs_e is the jump in specific entropy at the equilibrium temperature. It is a good approximation over a modest range of temperatures to take $\Delta \nu = 0$ and $A = A_0(\theta - \theta_c)$, $A_0 > 0$, where θ_c is the critical temperature at which stress-free A loses its thermodynamic stability. The resulting linear temperature dependence of ΔG^θ is in good agreement with experiments on shape memory alloys and some steels over a wide range of temperatures. Let $\bar{\theta}_c$ denote the critical temperature at which stress-free M loses its thermodynamic stability. From Eqs. (14) we obtain

$$\begin{aligned} A \rightarrow M: \quad &\theta \leq \theta_c, \\ M \rightarrow A: \quad &\theta \geq \bar{\theta}_c := \theta_c + \frac{6z(\theta_e - \theta_c)}{6z - A_0}, \quad A_0 < 6z. \end{aligned} \quad (16)$$

The inequality $A_0 < 6z$ follows from the obvious inequalities $\bar{\theta}_c > \theta_e > \theta_c$. It is often assumed that the equilibrium temperature is the average of the critical temperatures, but in fact there are no experimental data to support this supposition. Nevertheless, in that case we have $A_0 = 3z$,

$$\Delta G^\theta = A_0(\theta - \theta_e)/3,$$

$$f = A_0[(\theta - \theta_c)\eta^2 - 2(\theta + 2\theta_e - 3\theta_c)\eta^3/3 + (\theta_e - \theta_c)\eta^4]. \quad (17)$$

We now obtain a parametric representation of stress-strain curves for transformations that can be treated as one-dimensional, i.e., $\boldsymbol{\sigma} \cdot \boldsymbol{\varepsilon}_t = \sigma \varepsilon_t$, where σ and ε_t are scalar measures of stress and transformation strain. Four important examples of one-dimensional transformations are

$$\boldsymbol{\varepsilon}_t = \frac{1}{2} \gamma_t (\mathbf{m}\mathbf{n} + \mathbf{n}\mathbf{m}), \quad \varepsilon_t = \gamma_t, \quad \sigma = \tau := \mathbf{m} \cdot \boldsymbol{\sigma} \cdot \mathbf{n}; \quad (18)$$

$$\boldsymbol{\varepsilon}_t = \varepsilon \mathbf{n}\mathbf{n}, \quad \varepsilon_t = \varepsilon, \quad \sigma = \mathbf{n} \cdot \boldsymbol{\sigma} \cdot \mathbf{n}; \quad (19)$$

$$\boldsymbol{\varepsilon}_t = \frac{1}{3} \varepsilon_0 \mathbf{I}, \quad \varepsilon_t = \varepsilon_0, \quad \sigma = \frac{1}{3} \boldsymbol{\sigma} : \mathbf{I}; \quad (20)$$

$$\boldsymbol{\varepsilon}_t = \varepsilon \left(\mathbf{e}_1 \mathbf{e}_1 - \frac{1}{2} \mathbf{e}_2 \mathbf{e}_2 - \frac{1}{2} \mathbf{e}_3 \mathbf{e}_3 \right), \quad \varepsilon_t = \varepsilon,$$

$$\sigma = \mathbf{e}_1 \cdot \boldsymbol{\sigma} \cdot \mathbf{e}_1 - \frac{1}{2} \mathbf{e}_2 \cdot \boldsymbol{\sigma} \cdot \mathbf{e}_2 - \frac{1}{2} \mathbf{e}_3 \cdot \boldsymbol{\sigma} \cdot \mathbf{e}_3. \quad (21)$$

Equation (18) describes simple shear in direction \mathbf{m} in the shear plane with normal \mathbf{n} . The shear stress is τ and γ_t is the shear strain. Equation (19) describes simple tension (compression) in the \mathbf{n} direction. Equation (20) corresponds to a pure volumetric transformation strain ε_0 with mean stress (hydrostatic pressure) σ . Equation (21) describes a cubic to tetragonal transformation with elongation in the \mathbf{e}_1 direction and compensating contractions along the \mathbf{e}_2 and \mathbf{e}_3 directions. In all four cases, Eq. (12) for η_3 provides us with the equilibrium stress-transformation strain curve

$$\sigma = \frac{2(A - 3\Delta G^\theta) \eta - A}{\varepsilon_t [2(a - 3) \eta - a]}. \quad (22)$$

For $0 < a < 6$, the denominator of Eq. (22) is nonzero for $0 \leq \eta \leq 1$. Since the parameter η maximizes G , for each $\boldsymbol{\sigma}$ and θ , the equilibrium curve Eq. (22) is unstable. This is reflected by a decrease in σ with an increase in η . In the approximation that $\Delta \nu = 0$, the σ - η curve depends linearly on temperature

$$\sigma = \frac{2[A_0(\theta - \theta_c) - 3z(\theta - \theta_e)] \eta - A_0(\theta - \theta_c)}{\varepsilon_t [2(a - 3) \eta - a]}. \quad (23)$$

The stress hysteresis $H := \sigma(\eta = 0) - \sigma(\eta = 1)$ is given by

$$H = \frac{6}{\varepsilon_t} \frac{(A_0 - za)\theta + za\theta_e - A_0\theta_c}{a(6 - a)}, \quad (24)$$

which is independent of temperature, as in SMA and steels, for $A_0 = za$. Equations (22) [or (23)] and (8) constitute a parametric representation of the unstable branch of the equilibrium stress-strain curve. Stress-strain curves at several temperatures are shown in Fig. 5, where arrows indicate the strain jump at constant stress in a stress-controlled experiment. They agree qualitatively with the schematic stress-strain curves of Fig. 1. They exhibit the most important features of martensitic phase transitions in SMA, namely, temperature independent stress hysteresis and transformation

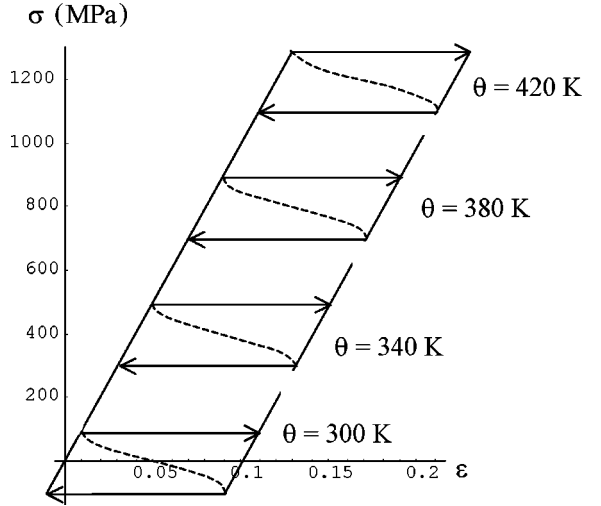


FIG. 5. Equilibrium stress-strain curves at various temperatures (designated near curves) for $\lambda = 10^{-4} \text{ MPa}^{-1}$, $\varepsilon_t = 0.1$, $a = 3$, $\theta_c = 290 \text{ K}$, $\theta_e = 300 \text{ K}$, and $A_0 = 3 \text{ MPa/K}$. Unstable regions are dashed.

strain and nonzero tangent moduli where A and M lose stability. The experimentally observed diagonal AD in Fig. 1 is described as well.

The parameters a and A do not affect thermodynamic equilibrium conditions, instead they characterize energy barriers. After ΔG^θ is determined from thermodynamic equilibrium conditions, the parameters θ_c and A_0 (or $\bar{\theta}_c$) can be determined from the $A \leftrightarrow M$ transition temperatures under stress-free conditions, and finally the parameter a can be determined from phase transformation condition (14) at various temperatures. The dependence of $\tilde{G} := G + \boldsymbol{\sigma} : \boldsymbol{\lambda} : \boldsymbol{\sigma} / 2$ on η is presented in Fig. 6.

B. η -dependent thermal strain and elastic compliances through fourth order

In order to account for nonzero thermal strain $\boldsymbol{\varepsilon}_\theta$ and changes in the elastic compliances through fourth order during the PT we define

$$\begin{aligned} G = & -\boldsymbol{\sigma} : \boldsymbol{\lambda}(\eta) : \boldsymbol{\sigma} / 2 - [\boldsymbol{\sigma} : \boldsymbol{\lambda}^3(\eta) : \boldsymbol{\sigma}] : \boldsymbol{\sigma} / 3 \\ & - \boldsymbol{\sigma} : [\boldsymbol{\sigma} : \boldsymbol{\lambda}^4(\eta) : \boldsymbol{\sigma}] : \boldsymbol{\sigma} / 4 - \boldsymbol{\sigma} : \boldsymbol{\varepsilon}_t \varphi(\eta) \\ & - \boldsymbol{\sigma} : \boldsymbol{\varepsilon}_\theta(\eta) + f(\theta, \eta), \end{aligned} \quad (25)$$

$$\boldsymbol{\lambda}^m(\eta) = \boldsymbol{\lambda}_0^m + (\boldsymbol{\lambda}_1^m - \boldsymbol{\lambda}_0^m) \varphi_{m\lambda}(\eta), \quad (26)$$

$$\begin{aligned} \boldsymbol{\varepsilon}_\theta(\eta) = & \boldsymbol{\varepsilon}_{\theta 0} + (\boldsymbol{\varepsilon}_{\theta 1} - \boldsymbol{\varepsilon}_{\theta 0}) \varphi_\theta(\eta), \quad \boldsymbol{\varepsilon}_{\theta 0} = \boldsymbol{\alpha}_0(\theta - \theta_0), \\ & \boldsymbol{\varepsilon}_{\theta 1} = \boldsymbol{\alpha}_1(\theta - \theta_0), \end{aligned} \quad (27)$$

where $\boldsymbol{\lambda}_0^m$ and $\boldsymbol{\lambda}_1^m$ are the m th order elastic compliances (rank $2m$ tensors) of A and M , $\boldsymbol{\lambda} := \boldsymbol{\lambda}_0^2$, $\boldsymbol{\alpha}_0$ and $\boldsymbol{\alpha}_1$ are the thermal expansion tensors of A and M , and θ_0 is some reference temperature, e.g., θ_e . As the functions $\varphi_{m\lambda}$ and φ_θ have to satisfy the same four conditions as φ , one obtains

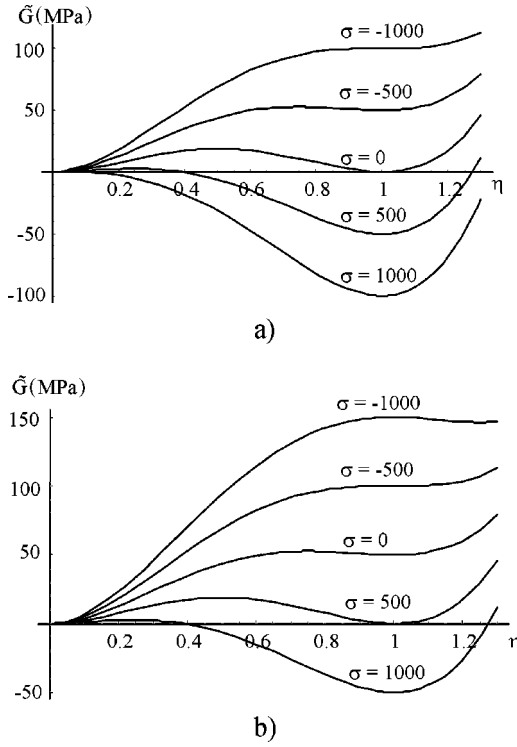


FIG. 6. $\tilde{G}(\eta)$ for equal deviations of the critical temperatures from the equilibrium temperature at various stresses (designated in MPa near curves) for (a) $\theta = 200$ K and (b) $\theta = 250$ K; $\varepsilon_t = 0.1$, $a = 3$, $\theta_c = 100$ K, $\theta_e = 200$ K, $A_0 = 3$ MPa/K.

$$\varphi_{m\lambda}(\eta) = a_{m\lambda}\eta^2 + (4 - 2a_{m\lambda})\eta^3 + (a_{m\lambda} - 3)\eta^4, \quad (28)$$

$$0 < a_{m\lambda} < 6,$$

$$\varphi_{\theta}(\eta) = a_{\theta}\eta^2 + (4 - 2a_{\theta})\eta^3 + (a_{\theta} - 3)\eta^4, \quad 0 < a_{\theta} < 6. \quad (29)$$

The difference between the Gibbs potentials of the A and M is

$$\begin{aligned} G(\boldsymbol{\sigma}, \theta, 0) - G(\boldsymbol{\sigma}, \theta, 1) &= \boldsymbol{\sigma} : \boldsymbol{\varepsilon}_t + \boldsymbol{\sigma} : (\boldsymbol{\varepsilon}_{\theta 1} - \boldsymbol{\varepsilon}_{\theta 0}) + \boldsymbol{\sigma} : (\boldsymbol{\lambda}_1 - \boldsymbol{\lambda}_0) : \boldsymbol{\sigma} / 2 \\ &+ [\boldsymbol{\sigma} : (\boldsymbol{\lambda}_1^3 - \boldsymbol{\lambda}_0^3) : \boldsymbol{\sigma}] : \boldsymbol{\sigma} / 3 \\ &+ \boldsymbol{\sigma} : [\boldsymbol{\sigma} : (\boldsymbol{\lambda}_1^4 - \boldsymbol{\lambda}_0^4) : \boldsymbol{\sigma}] : \boldsymbol{\sigma} / 4 - \Delta G^{\theta}. \end{aligned} \quad (30)$$

The solutions of the thermodynamic equilibrium condition $\partial G / \partial \eta = 0$ are

$$\eta_1 = 0, \quad \eta_2 = 1, \quad \eta_3 = \frac{1}{2}(A - \boldsymbol{\sigma} : \mathbf{h}_1) / (A - 3\Delta G^{\theta} - \boldsymbol{\sigma} : \mathbf{h}_2),$$

$$\begin{aligned} \mathbf{h}_1 &:= a\boldsymbol{\varepsilon}_t + a_{\theta}(\boldsymbol{\varepsilon}_{\theta 1} - \boldsymbol{\varepsilon}_{\theta 0}) + a_{\lambda}(\boldsymbol{\lambda}_1 - \boldsymbol{\lambda}_0) : \boldsymbol{\sigma} / 2 \\ &+ a_{3\lambda}\boldsymbol{\sigma} : (\boldsymbol{\lambda}_1^3 - \boldsymbol{\lambda}_0^3) : \boldsymbol{\sigma} / 3 + a_{4\lambda}[\boldsymbol{\sigma} : (\boldsymbol{\lambda}_1^4 - \boldsymbol{\lambda}_0^4) : \boldsymbol{\sigma}] : \boldsymbol{\sigma} / 4, \end{aligned}$$

$$\begin{aligned} \mathbf{h}_2 &:= (a - 3)\boldsymbol{\varepsilon}_t + (a_{\theta} - 3)(\boldsymbol{\varepsilon}_{\theta 1} - \boldsymbol{\varepsilon}_{\theta 0}) \\ &+ (a_{\lambda} - 3)(\boldsymbol{\lambda}_1 - \boldsymbol{\lambda}_0) : \boldsymbol{\sigma} / 2 + (a_{3\lambda} - 3)\boldsymbol{\sigma} : (\boldsymbol{\lambda}_1^3 - \boldsymbol{\lambda}_0^3) : \boldsymbol{\sigma} / 3 \\ &+ (a_{4\lambda} - 3)[\boldsymbol{\sigma} : (\boldsymbol{\lambda}_1^4 - \boldsymbol{\lambda}_0^4) : \boldsymbol{\sigma}] : \boldsymbol{\sigma} / 4. \end{aligned} \quad (31)$$

The conditions for the $A \rightarrow M$ and $M \rightarrow A$ PT, $\partial^2 G / \partial \eta^2 \leq 0$ at $\eta = 0$ and $\eta = 1$, respectively, are generalizations of Eq. (14)

$$\begin{aligned} A \rightarrow M: \quad &a\boldsymbol{\sigma} : \boldsymbol{\varepsilon}_t + a_{\theta}\boldsymbol{\sigma} : (\boldsymbol{\varepsilon}_{\theta 1} - \boldsymbol{\varepsilon}_{\theta 0}) + \frac{a_{\lambda}}{2}\boldsymbol{\sigma} : (\boldsymbol{\lambda}_1 - \boldsymbol{\lambda}_0) : \boldsymbol{\sigma} \\ &+ \frac{a_{3\lambda}}{3}\boldsymbol{\sigma} : [(\boldsymbol{\lambda}_1^3 - \boldsymbol{\lambda}_0^3) : \boldsymbol{\sigma}] : \boldsymbol{\sigma} \\ &+ \frac{a_{4\lambda}}{4}\boldsymbol{\sigma} : [\boldsymbol{\sigma} : (\boldsymbol{\lambda}_1^4 - \boldsymbol{\lambda}_0^4) : \boldsymbol{\sigma}] : \boldsymbol{\sigma} \geq A, \\ M \rightarrow A: \quad &(6 - a)\boldsymbol{\sigma} : \boldsymbol{\varepsilon}_t + (6 - a_{\theta})\boldsymbol{\sigma} : (\boldsymbol{\varepsilon}_{\theta 1} - \boldsymbol{\varepsilon}_{\theta 0}) \\ &+ \frac{6 - a_{\lambda}}{2}\boldsymbol{\sigma} : (\boldsymbol{\lambda}_1 - \boldsymbol{\lambda}_0) : \boldsymbol{\sigma} + \frac{6 - a_{3\lambda}}{3}\boldsymbol{\sigma} : [(\boldsymbol{\lambda}_1^3 - \boldsymbol{\lambda}_0^3) : \boldsymbol{\sigma}] : \boldsymbol{\sigma} \\ &+ \frac{6 - a_{4\lambda}}{4}\boldsymbol{\sigma} : [\boldsymbol{\sigma} : (\boldsymbol{\lambda}_1^4 - \boldsymbol{\lambda}_0^4) : \boldsymbol{\sigma}] : \boldsymbol{\sigma} \leq 6\Delta G^{\theta} - A. \end{aligned} \quad (32)$$

They are consistent with the conditions for the disappearance of activation barriers: $\eta_3 = \eta_1$ and $\eta_3 = \eta_2$. For temperature-induced PT ($\boldsymbol{\sigma} = \mathbf{0}$), Eqs. (16) remain valid.

The tensors $\boldsymbol{\lambda}_0^m$, $\boldsymbol{\lambda}_1^m$, $\boldsymbol{\alpha}_0$, and $\boldsymbol{\alpha}_1$ are assumed to be known. As before, ΔG^{θ} is determined from thermodynamic equilibrium conditions, and the parameters θ_c and A_0 (or $\bar{\theta}_c$) can be determined from the $A \leftrightarrow M$ PT temperatures under stress-free conditions. If the stresses for forward and reverse phase transformations are determined experimentally at various temperatures then the parameters a , $a_{m\lambda}$, and a_{θ} , which control the energy barrier between A and M but not thermodynamic equilibrium, can be obtained from Eq. (32). If a , a_{λ} , and a_{θ} are functions of temperature then they are not uniquely determined by conditions (32). One can model zero tangential moduli at PT points, if necessary.

III. CONCLUDING REMARKS

In part I, a three-dimensional Landau theory for stress- and temperature-induced $A \leftrightarrow M$ PT has been developed. In contrast to previous approaches, our theory allows for inclusion of all temperature-dependent thermomechanical properties of both phases and describes typical stress-strain curves with constant transformation strain tensors (temperature and stress independent), constant or weakly temperature dependent stress hysteresis, and transformation at nonzero tangent moduli. The free energy polynomial is sufficiently simple that spurious extrema do not appear.

Martensitic PT for which the leading transformation mode is a transformation strain (the case considered in this paper) are classified as proper PT according to Ref. 5. For proper PT, the transformation strain is linearly dependent on the order parameter. For improper PT, in which the soft optical displacement mode is a primary transformation mode and

transformation strain is a secondary effect, the transformation strain is at least quadratic in the order parameters. Such a classification scheme is not satisfactory because, as we have shown, martensitic PT for which the leading mode is transformation strain have a 2-3-4 polynomial dependence of transformation strain on the order parameter. Note that the order parameter is not a small parameter so a higher degree polynomial does not mean a weaker effect. Maybe the term “strong” martensitic PT for the PT with transformation strain as a leading mode in contrast to “weak” PT for the case when transformation strain is a secondary effect would be more suitable.

We see no way to describe all of the desirable features of strong martensitic PT using a polynomial in the total strain rather than a polynomial in order parameters related to the transformation strain. It would be quantitatively incorrect to determine barriers for the $A \leftrightarrow M$ PT or the variant-variant PT (in part II) from experimental stress-strain curves for single crystals. Stress-strain curves are strongly affected by various defect distributions, surface energy, and the presence of a fine twinned microstructure. Actual stresses in transforming material may be very different from applied stresses due to internal stresses induced by a heterogeneous distribution of transformation strain. Atomistic calculations are the best way to determine transformation barriers in our theory. Comparison with experimental stress-strain curves can be made after solution of the corresponding boundary-value problem with some prescribed (or determined by corresponding evolution equations) defect distribution.

Our Landau theory captures the main features of macroscopic stress-strain curves notwithstanding the effects of the microstructure. The transformation strain tensor (when twin-

ning is not involved, in particular, for the pseudoelastic regime) and nonzero tangent elastic moduli are independent of the above factors and are defined by deformation of the crystal lattice. Stress hysteresis is strongly affected by defects so we cannot exclude the possibility that defects change its temperature dependence. Dislocation structure does not evolve significantly during PT in the temperature range of interest; the PT itself is the dominant mechanism of plasticity. Thus we expect dislocations to change stress hysteresis by approximately the same value at any temperature. But the main point is that even if this is not the case, our theory is flexible enough to employ any temperature dependence for the stress hysteresis.

Twinning can substantially increase the pseudoplastic stress hysteresis relative to the pseudoelastic stress hysteresis. This behavior is not predicted by our Landau potential; it is necessary to solve the corresponding boundary value problem (see Ref. 33).

Our Gibbs potential for the $A \leftrightarrow M$ PT can be used to describe twinning and transformations between martensitic variants. Twinning can be regarded as the special case of our $A \leftrightarrow M$ PT theory where the jump in the thermal part of the free energy is set of zero and the transformation strain corresponds to simple shear. Transformations between variants can be modeled by taking $\Delta G^\theta = 0$ and accounting for the nonzero transformation strain of the initial variant.

ACKNOWLEDGMENTS

The support of Los Alamos National Laboratory for V.I.L. under consulting agreement C-8060 is gratefully acknowledged. The technical assistance of Dong-Wook Lee (Texas Tech University) is very much appreciated.

*Email address: valery.levitas@coe.ttu.edu

¹L.D. Landau, Zh. Eksp. Teor. Fiz. **7**, 19 (1937); **7**, 627 (1937); translation in *Collected Papers of L. D. Landau*, edited by D. Ter Haar (Pergamon Press, Oxford, 1965), pp. 193, 216.

²P. Toledano and V. Dmitriev, *Reconstructive Phase Transitions* (World Scientific, New Jersey, 1996).

³Y. Wang and A.G. Khachaturyan, Acta Mater. **45**, 759 (1997).

⁴A. Artemev, Y. Wang, and A.G. Khachaturyan, Acta Mater. **48**, 2503 (2000).

⁵A. Artemev, Y. Jin, and A.G. Khachaturyan, Acta Mater. **49**, 1165 (2001).

⁶T. Ichitsubo, K. Tanaka, M. Koiwa, and Y. Yamazaki, Phys. Rev. B **62**, 5435 (2000).

⁷C. M. Wayman, *Introduction to the Crystallography of Martensitic Transformation* (Macmillan, New York, 1964).

⁸J. C. Toledano and P. Toledano, *The Landau Theory of Phase Transitions* (World Scientific, Singapore, 1988).

⁹E. K. H. Salje, *Phase Transitions in Ferroelastic and Co-Elastic Crystals* (Cambridge University Press, New York, 1990).

¹⁰K. Bhattacharyya and R.V. Kohn, Acta Mater. **4**, 529 (1996).

¹¹E. I. Estrin, in *Phase Transformation of Martensitic Type*, edited by V. V. Nemozhkalkenko (Naukova Dumka, Kiev, 1993), pp. 110–139.

¹²A. Planes, Ll. Manosa, and E. Vives, J. Phys. III **5**, 173 (1995).

¹³S. Fu, Y. Huo, and I. Müller, Acta Mech. **99**, 1 (1993).

¹⁴J.A. Shaw, Int. J. Plast. **16**, 541 (2000).

¹⁵C. Zener, Phys. Rev. **7**, 846 (1947).

¹⁶T.A. Schröder and C.M. Wayman, Acta Metall. **27**, 405 (1979).

¹⁷H. Pops, Metall. Trans. **1**, 251 (1970).

¹⁸F. Falk, Arch. Mech. **15**, 63 (1983).

¹⁹A. Saxena, Y. Wu, T. Lookman, S.R. Shenoy, and A.R. Bishop, Physica A **239**, 18 (1997).

²⁰S.R. Shenoy, T. Lookman, A. Saxena, and A.R. Bishop, Phys. Rev. B **60**, R12 537 (1999).

²¹G. B. Olson and M. Cohen, in *Dislocations in Solids*, edited by F. R. N. Nabarro (Elsevier Science Publishers, Amsterdam, 1986), Vol. 7, pp. 297–407.

²²B. Moran, Y.A. Chu, and G.B. Olson, Int. J. Solids Struct. **33**, 1903 (1996).

²³G.R. Barsch and J.A. Krumhansl, Phys. Rev. Lett. **53**, 1069 (1989).

²⁴G. R. Barsch and J. A. Krumhansl, in *Martensite*, edited by G. B. Olson and W. S. Owen (ASM International, Materials Park, OH, 1992), pp. 125–147.

²⁵P.A. Lindgård and O.G. Mouritsen, Phys. Rev. Lett. **57**, 2458 (1986).

²⁶V.G. Bar'yachtar, S.G. Enilevskiy, V.V. Tokiy, and D.A. Jablonsky, Sov. Phys. Solid State **28**, 1303 (1986).

²⁷A.A. Boulbitch and P. Toledano, Phys. Rev. Lett. **81**, 838 (1998).

²⁸R.J. Gooding and J.A. Krumhansl, Phys. Rev. B **38**, 1695 (1988).

- ²⁹R.J. Gooding and J.A. Krumhansl, Phys. Rev. B **39**, 1535 (1989).
- ³⁰R.J. Gooding, Y.Y. Ye, C.T. Chan, K.M. Ho, and B.N. Harmon, Phys. Rev. B **43**, 13 626 (1991).
- ³¹P.C. Clapp, C.S. Besquart, Y. Shao, Y. Zhao, and J.A. Rifkin, Modell. Simul. Mater. Sci. Eng. **2**, 551 (1994).
- ³²F. Falk and P. Konopka, J. Phys.: Condens. Matter **2**, 61 (1990).
- ³³V. I. Levitas and D. L. Preston, following paper, Phys. Rev. B **66**, 134207 (2002).
- ³⁴Y.H. Wen, Y. Wang, and L.Q. Chen, Acta Mater. **47**, 4375 (1999).
- ³⁵R. Abeyaratne, C. Chu, and R.D. James, Philos. Mag. A **73**, 457 (1996).
- ³⁶V.I. Levitas, Int. J. Solids Struct. **35**, 889 (1998).
- ³⁷V. I. Levitas, *Large Deformation of Materials with Complex Rheological Properties at Normal and High Pressure* (Nova Science Publishers, New York, 1996).